An Investigation into the Geometric Parameters Affecting Field Uniformity in Four Pole Magnetisers

James Borg Bartolo[1], Piotr Klimczyk[2], Kai Tiwisina[2], Patrick Denke[2], Stefan Siebert[2], Christopher Gerada[1]
[1]*University of Nottingham, NG72RD Nottingham UK,*
[2]*Dr. Brockhaus Messstechnik GmbH & Co. KG, D-58507 Lüdenscheid Germany*

Abstract. In recent years, the field-metric method for measuring the joule losses set up in an electrical steel laminate when subjected to a rotating field has gained popularity. The ideal geometry of the magnetiser required to set up such a field is still however the subject of much debate. The work presented here aims at providing some useful guidelines which might be considered when undertaking the construction of the simplest of such magnetizing setups having four salient poles excited by a two phase system and using a square sample. A 3D model for this rotational power loss tester was simulated for different pole geometries with the induction uniformity being assessed for every alteration.

I. Model geometry and simulation setup

To cater for the affects of pole tapering, pole-yoke air gaps and the proper location of the sample plane (x-y) with respect to the pole tip, in the z dimension, a 3D model of the magnetising yoke was setup as shown in Figure 1(a) with the salient pole parameters shown in Figures 1(b, c, d) for different projections.

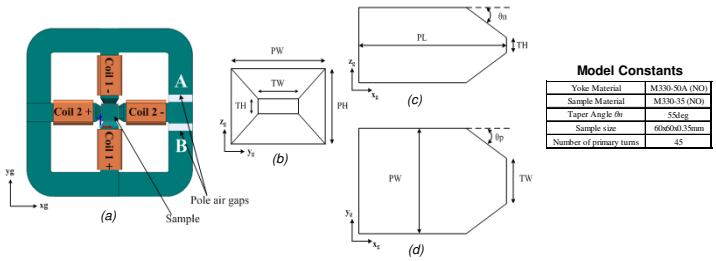

Model Constants

Yoke Material	M330-50A (NO)
Sample Material	M330-35 (NO)
Taper Angle θ_{tt}	55deg
Sample size	60x60x0.35mm
Number of primary turns	45

Fig.1 (a) Magnetising yoke geometry in full plan view including the introduction of the parasitic air gaps at the pole-yoke interface, (b) frontal projection of a pole tip, (c) side elevation of a pole tip and (d) plan view of a pole tip

II. Criteria for assessing induction uniformity

The proposed variations to the pole geometry were assessed on the basis of their affect on the induction uniformity within the sample. Such uniformity was assessed globally, using a rate of change criterion, whilst locally; the deviation of edge and corner induction values from the sample's mean induction value, evaluated in the area enclosed by the measuring coils, was employed.

A. The mean rate-of-change criterion

$$M_{Byx} = \frac{1}{m}\left[\frac{B[i,2]-B[i,1]}{\Delta y} - \sum_{k=2}^{m}\frac{B[i,k]-B[i,k-1]}{\Delta y}\right] = \left[\frac{\overline{\Delta B}}{\Delta y}\Big|_{x[1]}, \frac{\overline{\Delta B}}{\Delta y}\Big|_{x[2]}, \frac{\overline{\Delta B}}{\Delta y}\Big|_{x[3]} \cdots \frac{\overline{\Delta B}}{\Delta y}\Big|_{x[i]}\right]$$

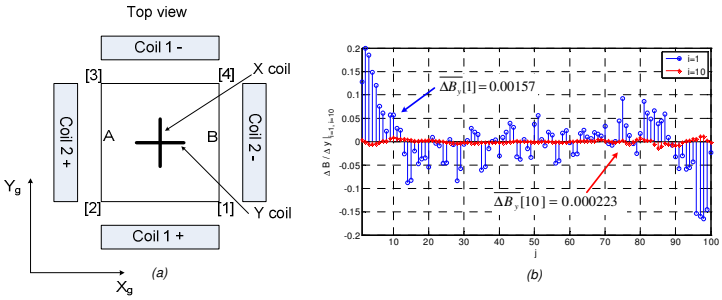

Fig.2 (a) Reference system used, (b) Variation of finite differences against sample number along the y_g direction

B. The Induction deviation criteria

$$\varepsilon_e = \frac{\mathbf{B}_y[i]-B_{ca}}{B_{ca}}; \quad i=1,n$$

$$\varepsilon_{rc} = \frac{\mathbf{B}[i,j]-B_{ca}}{B_{ca}}; \quad i=1,n \;;\; j=1,m$$

$$\varepsilon_m(x,y) = \frac{\mathbf{B}[i,j]-B_{ca}}{B_{ca}}; \quad i=1,..n \;;\; j=1,...m$$

where:
ε_e is the deviation at the sample edges,
ε_{rc} is the deviation at the sample corners,
ε_m is the deviation at the surface,
B[i,j] is the induction matrix,
B_{ca} is the induction level averaged over the coil aperture area.

III. Results

Case number	Laminate orientation	Tip width	Side taper	Coil aperture	Sample airgap	Pole aigaps A	Pole aigaps B	Excitation current	B_{ca}	$\|M_{Byx}\|$	Standard Deviation for M_{Byx}	Deviation at sample Edge A	Deviation at sample Edge B	Deviation at the sample corners ε_{rc} 1	2	3	4
		mm	*Deg*	*mm*	*mm*	*mm*	*mm*	*Amps*	*Tesla*			ε_e	ε_e				
1	Orthogonal	45	0	24	3	0	0	1.88	0.82	6.36E-06	0.000	-0.531	-0.533	-0.600	-0.615	-0.594	-0.626
2	Parallel	45	0	24	3	0	0	1.88	0.83	6.52E-06	0.000	-0.531	-0.534	-0.598	-0.614	-0.592	-0.624
3	Orthogonal	45	0	24	3	0	0	18.20	1.82	1.36E-05	0.000	-0.036	-0.038	-0.084	-0.105	-0.104	-0.114
4	Parallel	45	0	24	3	0	0	18.20	1.82	1.38E-05	0.000	-0.036	-0.037	-0.082	-0.103	-0.102	-0.112
5	Orthogonal	45	0	24	1	0	0	1.88	1.16	1.75E-05	0.000	-0.324	-0.333	-0.693	-0.670	-0.693	-0.672
6	Orthogonal	60	0	24	1	0	0	1.88	1.15	1.20E-04	0.000	-0.487	-0.479	-0.249	-0.351	-0.250	-0.250
7	Orthogonal	45	0	24	1	0	0	18.20	1.83	2.44E-05	0.000	-0.033	-0.028	-0.200	-0.195	-0.196	-0.200
8	Orthogonal	60	0	24	1	0	0	18.20	1.83	4.24E-05	0.000	-0.029	-0.022	0.150	0.147	0.146	0.159
1	Orthogonal	45	0	24	3	0	0	1.88	0.82	6.36E-06	0.000	-0.531	-0.533	-0.600	-0.615	-0.594	-0.626
9	Orthogonal	45	60	24	3	0	0	1.88	0.83	2.30E-05	0.000	-0.534	-0.536	-0.573	-0.582	-0.563	-0.605
10	Orthogonal	45	45	24	3	0	0	1.88	0.82	9.31E-07	0.000	-0.529	-0.536	-0.555	-0.561	-0.543	-0.595
11	Orthogonal	60	0	24	3	0	0	1.88	0.86	5.11E-06	0.000	-0.516	-0.520	-0.416	-0.394	-0.411	-0.474
12	Orthogonal	60	60	24	3	0	0	1.88	0.85	1.23E-05	0.000	-0.512	-0.520	-0.407	-0.391	-0.420	-0.473
13	Orthogonal	60	45	24	3	0	0	1.88	0.83	4.45E-05	0.000	-0.514	-0.522	-0.413	-0.349	-0.416	-0.461
5	Orthogonal	45	0	24	1	0	0	1.88	1.16	1.75E-05	0.000	-0.324	-0.333	-0.693	-0.670	-0.693	-0.672
14	Orthogonal	45	0	28	1	0	0	1.88	1.10	5.36E-06	0.000	-0.489	-0.480	-0.753	-0.725	-0.757	-0.714
15	Orthogonal	45	0	32	1	0	0	1.88	1.10	2.16E-06	0.000	-0.489	-0.475	-0.754	-0.724	-0.753	-0.712
7	Parallel	45	0	24	1	0	0	18.20	1.83	2.44E-05	0.000	-0.033	-0.028	-0.200	-0.195	-0.196	-0.200
PAG	Parallel	45	0	24	1	0.5	0.5	18.20	1.77	3.04E-05	0.000	-0.042	-0.040	-0.202	-0.231	-0.194	-0.201
PAG_asym	Parallel	45	0	24	1	0.5	0.25	18.20	1.77	2.47E-05	0.000	-0.042	-0.039	-0.200	-0.231	-0.196	-0.198

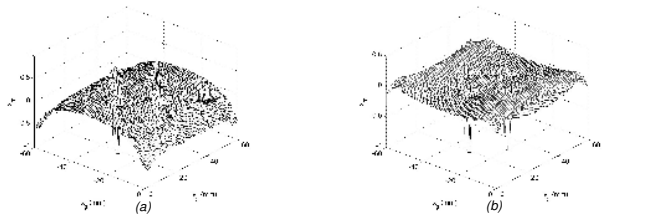

Fig.3 Surface plot showing the deviation in sample induction from the mean value for: (a) case 1 with pole laminates orthogonal to the sample plane and B_{ca}=0.82T, (b) case 3 with pole laminates orthogonal to the sample plane and B_{ca}=1.82T

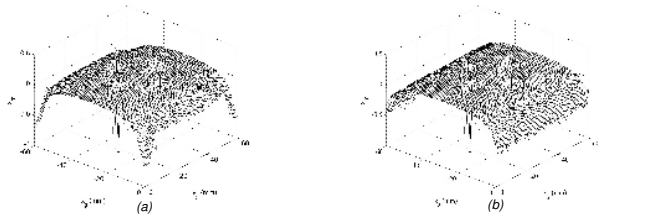

Fig.4 Surface plot showing the deviation in sample induction from the mean value for: (a) case 5 with tip width at 45 mm and B_{ca}=1.16T, (b) case 6 with tip width equal to sample width and B_{ca}=1.15T

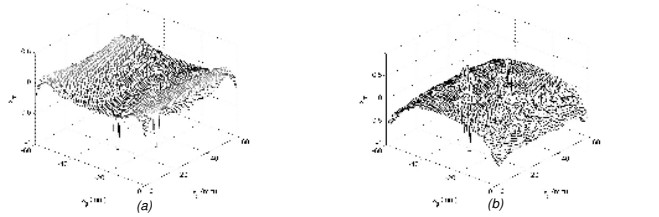

Fig.5 Surface plot showing the deviation in sample induction from the mean value for: (a) case 7 having a tip width of 45 mm, no pole air-gaps and B_{ca}=1.83T, (b) case PAG with tip width at 45 mm, symmetric pole air gaps and B_{ca}=1.77T

IV. Conclusion

By considering the Mean rate of change criterion, M_{Bxy}, and the mean induction deviation criteria, the following conclusions can be drawn flowing from the results presented above:

i) Induction uniformity is largely unaffected by the pole laminate orientation, where the sample air gap is larger than 1 mm, ref. cases 1, 2, 3 and 4.
ii) For a sample air gap of 1 mm a Tip width of 45 mm will result in the best global induction uniformity, however at low induction values local induction deviations for such geometry exceed those presented by the 60 mm case (ref. cases 5, 6, 7, and 8). If a large sample air-gap were to be considered, than the 60 mm tip width provides for better uniformity (ref. cases 1 and 11).
iii) Cases 5 and 1, confirm that a larger air gap leads to better induction uniformity, at the cost of reduced mean magnitude, with 1.15T and 0.82T respectively.
iv) From cases 1, 9-10, it can be seen that introducing a 45 degree side taper can help uniformity, (ref. case 1 and 10) for the case in which a 45 mm tip width is considered with a 3 mm air gap. Otherwise such a feature does not greatly enhance uniformity.
v) From cases 5, 14, 15, it can be seen that the B-sensing coil aperture is critical in through-hole setups. With increasing levels of uniformity being obtained for increasing coil apertures.
vi) Introducing pole air gaps reduces the mean induction value; this however, is also accompanied by a reduction in uniformity. Also it should be noted that for cases PAG, PAG_asym, corner 3, (lying opposite to the introduced gaps), exhibits the lowest deviation from the mean induction level due to the experienced increased flux leakage as expected.

The University of Nottingham

2dm Torino 2014

BROCKHAUS MEASUREMENTS